BJR

https://doi.org/10.1259/bjr.20200287

Received: 27 March 2020 | Revised: 14 July 2020 | Accepted: 18 August 2020

Cite this article as:
Bian T, Wu Z, Lin Q, Wang H, Ge Y, Duan S, et al. Radiomic signatures derived from multiparametric MRI for the pretreatment prediction of response to neoadjuvant chemotherapy in breast cancer. *Br J Radiol* 2020; **93**: 20200287.

FULL PAPER

Radiomic signatures derived from multiparametric MRI for the pretreatment prediction of response to neoadjuvant chemotherapy in breast cancer

[1]TIANTIAN BIAN, [2]ZENGJIE WU, [1]QING LIN, [1]HAIBO WANG, [3]YAQIONG GE, [3]SHAOFENG DUAN, [4]GUANGMING FU, [1]CHUNXIAO CUI and [1]XIAOHUI SU

[1]Breast Disease Center, The Affiliated Hospital of Qingdao University, Qingdao 266000, Shandong, China
[2]Department of Radiology, The Affiliated Hospital of Qingdao University, Qingdao 266000, Shandong, China
[3]GE Healthcare, Pudong, 210000, Shanghai, China
[4]Department of Pathology, The Affiliated Hospital of Qingdao University, Qingdao 266000, Shandong, China

Address correspondence to: Dr Qing Lin
E-mail: *linqing_9180@163.com*

The authors Tiantian Bian and Zengjie Wu contributed equally to the work.

Objectives: To investigate the ability of radiomic signatures based on MRI to evaluate the response and efficiency of neoadjuvant chemotherapy (NAC) for treating breast cancers.
Methods: 152 patients were included in this study at our institution between March 2017 and September 2019. All patients with breast cancer underwent a preoperative breast MRI and the Miller–Payne grading system was applied to evaluate response to NAC. Quantitative parameters were compared between patients with sensitive and insensitive responses to NAC and between those with pathological complete responses (pCR) and non-pCR. Four radiomic signatures were built based on T2W imaging, diffusion-weighted imaging, dynamic contrast-enhanced imaging and their combination, and radiomics scores (Rad-score) were calculated. The combination of the clinical factors and Rad-scores created a nomogram model. Multivariate logistic regression was performed to assess the association between MRI features and independent clinical risk factors.
Results: 20 features and 18 features were selected to build the radiomic signature for evaluating sensitivity and the possibility of pCR, respectively. The combined radiomic signature and nomogram model showed a similar discrimination in the training (AUC 0.91, 0.92, 95% confidence interval [CI], 0.85–0.96, 0.86–0.98) and validation (AUC 0.93, 0.91, 95% CI, 0.86–1.00, 0.82–1.00) sets. The clinical factor model exhibited reduced performance (AUC 0.74, 0.64, 95% CI, 0.64–0.84, 0.46–0.82) in terms of NAC sensitivity and pCR.
Conclusions: The combined radiomic signature and nomogram model exhibited potential predictive power for predicting effective NAC treatment which can aid in the prognosis and guidance of treatment regimens.
Advances in knowledge: Identifying a means of assessing the efficacy of NAC before surgery can guide follow-up treatment and avoid chemotherapy-induced toxicity.

INTRODUCTION

Breast cancer has become the second leading cause of death among females all over the world[1–3] and some patients exhibit locally advanced breast cancer (LABC) that is either inoperable or requires extended radical resection which may eliminate the opportunity for breast-conserving or general surgery. Neoadjuvant chemotherapy (NAC) has been established as the standard treatment for patients with LABCs and can reduce the tumor burden, determine drug sensitivity and increase the rate of breast-conserving surgery.[4–8] These effects all contribute to the possibility of using surgical treatment for advanced-stage cancer. Currently, it has been identified that the majority of patients would benefit from NAC and some may even achieve pathological complete responses (pCR) due to NAC.[9] Previous studies have demonstrated that achieving pCR is associated with improved disease-free survival.[10] However, success rates for NAC vary based on the molecular subtype of the breast cancer and are highest in HER2 over expression and triple negative breast cancers.[11] The overall response rate to NAC ranges from 69 to 100% and approximately 30% of all patients do not respond to NAC. Furthermore, it is

estimated that up to 5% of patients experience disease progression after NAC and must bear the burden of various side-effects and the expensive cost of NAC with little benefit.[12,13] For these patients, NAC often simply delays surgical treatment rather than providing therapeutic value. In effect, the accurate evaluation of treatment efficacy and prognosis is essential in clinical practice for individualized medicine. It is therefore paramount to identify a means of assessing the efficacy of NAC that would facilitate the guidance of treatment regimens and avoid chemotherapy-induced toxicity.

Magnetic resonance imaging (MRI) is recommended by most experts for assessing the response to high-grade HER2 over expression and triple negative breast cancers as the accuracy for these subtypes is high, whereas accuracy is much lower when assessing the response to low-grade tumors and luminal cancers.[14] Significant advancements in medical image analysis and data mining have drawn attention to radiomics as an emerging technology for non-invasively profiling tumors within the field of oncology.[15–17] Radiomics relies on the extraction of mathematical patterns hidden in medical images and the conversion of these patterns into high-dimensional, quantitative features that represent underlying characteristics about the tumor.[18,19] Several prior studies have demonstrated that the response to NAC is associated with radiomic signatures derived from pre-treatment MRI; however, these studies used a small clinical sample size or focused on a particular MRI sequence or certain state of NAC response, such as pCR or insensitivity.[20] Hence, further validation is required to determine whether radiomics can provide sufficient evidence for the accurate estimation of NAC treatment benefit, risk of local recurrence, distant metastasis and prediction of prognosis. In our study, we utilized a large dataset that allowed for the comprehensive evaluation of various aspects of the MRI, including the size, shape, intensity, and enhancement of the tumor, changes to the texture of the surrounding tissue as well as the status of axillary lymph nodes.

Overall, the purpose of our study was to investigate the association between NAC treatment benefits and radiomic signatures from pre-treatment MR images and to estimate the clinical value of such signatures for the accurate prediction of the NAC treatment response.

METHODS AND MATERIALS

This retrospective study was approved by the Institutional Review Board of the Affiliated Hospital of Our University and written informed consent was provided by all individuals before participation.

Patients

We enrolled 247 patients who underwent MRI examinations between March 2017 and September 2019 at our institution. The study inclusion criteria were as follows: (1) biopsy-proven initial invasive breast cancer; (2) pre-treatment breast MRI examinations performed at our institution; (3) completion of the whole course of NAC treatment without any other treatment before surgery; (4) post-operative pathological evaluation using the Miller-Payne grading system. The exclusion criteria were as follows: (1) malignancy found in other organs, regardless of metastasis of the primary tumor; (2) lack of complete MR images before biopsy and NAC treatment; (3) any other treatment except for NAC before surgery; (4) missing surgical record or pathological evaluation at our institution. After the application of these criteria, 152 patients (mean age: 49 years, range: 28 to 69 years) were included in our study. We then randomly divided these patients into two cohorts; 107 patients were randomly allocated to the primary cohort and 45 were allocated to the validation cohort according to seed points set when programming. There was no significant difference between the training data and validation data.

MR imaging

For each patient, a pre-treatment breast MR examination and final pre-surgery MR examination were performed using a 3.0T (Signa HDxt, GE Healthcare) scanner equipped with a dedicated 8-channel or 16-channel breast coil. Patients were oriented in the prone position. MRI protocols consisted of an axial fat-suppressed T2W sequence (T2WI) by using an efficient method of water fat separation, a diffusion-weighted sequence (DWI), and a dynamic contrast-enhanced (DCE) fat-suppressed T1W sequence, consisting of earlier- and late-enhanced sequences. DWI images were obtained using 2 b-values (0 and 1000 s/m^2), while DCE images were collected with an i.v. injection of 0.2 ml/kg of Gadolinum-DTPA. The first post-contrast images were collected 60 s later when the injection of gadolinum-DTPA was initiated, and then seven subsequent scans were acquired. The temporal resolution of the DCE sequence was 65 s. Various parameters of different sequences of MRI are shown in Supplementary Material 1.

Conventional MRI evaluation and immunochemistry

All pre-treatment MR images were retrospectively analyzed by two board-certified radiologists with 6 and 30 years of experience in breast imaging according to the American College of Radiology Breast Imaging Reporting and Data System (ACR BI-RADS). Both radiologists were blinded to the pathological outcomes and assessed the following characteristics of each tumorous mass: shape (oval, round or irregular), margin (circumscribed, irregular or speculated), and internal enhancement characteristics (homogeneous, heterogeneous or rim) of each mass and the surrounding tissue. In addition, the minimum diameter of the lymph nodes was also assessed by the radiologists.

The gold standard is a histopathological assessment of the response to NAC treatment. Histochemical results of biopsy tissue were obtained to evaluate the concentration of estrogen receptor (ER), progesterone receptor (PR), Ki67 and human epidermal growth factor receptor2 (HER2). <1% of positive tumor cells with stained nuclei were considered ER/PR negative, while ≥1% were considered ER/PR positive. The cut-off value for Ki67 was set at 20%. For HER2, immunohistochemistry (IHC) scores of 3 + were considered HER2 positive, while scores of 0 and 1 + were considered HER2 negative. When the HER2 IHC score was 2+, further confirmation using fluorescence *in situ* hybridization (FISH) tests was required. Amplified results were

Figure 1. The radiomics feature selection using the least absolute shrinkage and selection operator (LASSO) regression model. (a) Selection of tuning parameter (λ) for NAC sensitivity in the LASSO model via a ten-fold cross-validation based on a minimizing criterion. The vertical black lines define the optimal values of λ; a λ value of 0.067 with log (λ)= - 4.999 was selected. (b) LASSO coefficient profiles for texture features. The vertical line is plotted with 20 radiomics features versus the selected log(λ) value via a ten-fold cross-validation. (c) Selection of the tuning parameter (λ) for the probability of achieving pCR in the LASSO model via a ten-fold cross-validation based on minimizing criteria. The vertical black lines define the optimal value of λ, a value λ of 0.021 with log (λ)= - 3.880 was selected. (d) LASSO coefficient profiles of texture features. The vertical line is plotted with 17 radiomics features versus the selected log(λ) value via a ten-fold cross-validation.

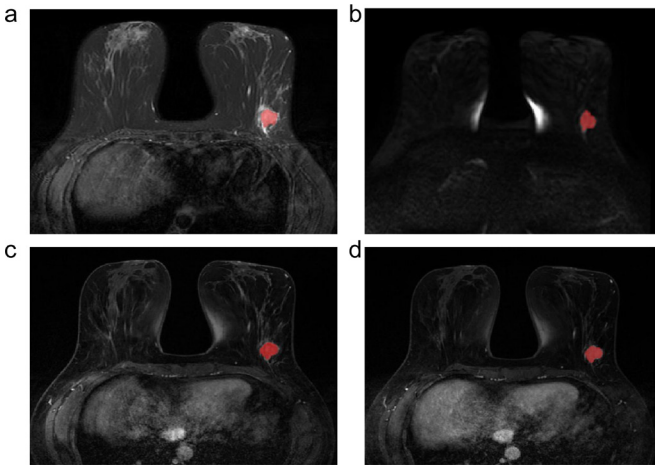

defined as HER2 positive and non-amplified results were defined as HER2 negative.

Construction of the clinical factor model

We combined age and MRI findings to create a clinical factor model. Univariate logistic regression analysis was used to compare the differences among such relative factors as age and MRI findings (tumor size, number of tumors, morphology of tumor, time intensity curve (TIC), the minimum diameter of axillary lymph node). TIC analysis was performed using the image processing workstations. The clinical prediction model was then constructed and evaluated via multiple logistic regression using optimal variables from the individual univariate analyses.

NAC treatment regimen and pathological assessment of response

All patients received six or eight cycles of NAC treatment before surgery. Different NAC treatment regimens were used according to their immunohistochemistry results. All protocols and timelines abided by the National Comprehensive Cancer Network (NCCN) guidelines. 87 patients (57.2%) received taxane-based regimens of six cycles and 65 patients (42.8%) received anthracycline- and taxane-based regimens of eight cycles. Patients with HER2 over expression also received trastuzumab (Herceptin; 8 mg/kg loading dose, 6 mg/kg maintenance dose). All patients underwent surgical resection 2–3 weeks after NAC treatment. A sentinel lymph node biopsy was performed for all patients using a fluorescent labeling method, whereas axillary nodal clearance was performed only for those with sentinel-node involvement.

All surgically resected specimens and lymph nodes were processed for standard histopathological assessment of response to NAC treatment. Two pathologists who were blinded to the outcomes of MRI and other patient characteristics evaluated the results. We assessed the benefit of NAC according to the Miller-Payne grading system. Grade one represents a pathological non-response to NAC with no overall reduction in the number of tumor cells (some minor alterations may be found in individual malignant cells). Grade two indicates a partial pathological response with the loss of less than 30% of tumor cells. Grade three indicates that more than 30% but less than 90% of the tumor cells are lost. Grade four indicates a loss of more than 90% of tumor cells. Grade five suggests pCR which was defined as the absence of residual invasive carcinoma in the specimen and the absence of invasive lesions in the lymph nodes, including the ipsilateral sentinel node and those from axillary dissections. Nevertheless, residual ductal carcinoma *in situ* can still be present. Overall, Grades 1–4 were classified as non-pCR, Grades 1–2 as insensitive to NAC and Grades 3–5 as sensitive to NAC, which suggested that those patients with Grades 1–2 would benefit less from NAC and would alternatively likely need surgery as a primary treatment.

Preparation for radiomics and feature extraction

MR images of DICOM format were loaded into the ITK-SNAP software (v., 3.4, www.itksnap.org) for further radiomics analysis. A region of interest (ROI), which was drawn separately for all sequences, was segmented manually in the largest cross-sectional area of the lesion and included the cystic components of the tumor (Figure 1). The ROIs were defined on the initial (Phase I) and delayed (lag Phase) enhanced sequences. The ROI was drawn as large as possible but did not include edge voxels to avoid partial volume effects. The mean intensity of the ROI was 31.60 (range: 23.44–44.83). Feature extraction was then performed using the AK platform (GE healthcare, v. 3.2.0). Intra- and inter-class correlation coefficients (ICCs) were used to assess the reproducibility and reliability of intra-observer results for feature extraction. Every radiologist repeated the same procedure 1 month later to evaluate the agreement between the features that were extracted at the two time points. The agreement was considered good with an ICC greater than 0.75. A total of 396 radiomics features were extracted based on ROIs.

Construction of radiomic signatures

Hundreds of features were extracted from the images and dimension reduction was performed on the feature set before constructing the radiomic signature. Redundant features were removed and the most meaningful features were identified to avoid overfitting. We used two feature selection methods, minimum redundancy maximum relevance (mRMR) and least absolute shrinkage and selection operator (LASSO), to select the feature. First, mRMR was performed to remove redundant and irrelevant features and effectively reduced the feature set down

Table 1. Clinical and pathological characteristics of pCR and non-pCR patients in the test and training cohort

	Test cohort		*p*	Training cohort		*p*
	pCR	Non-pCR		pCR	Non-pCR	
Amount	11	34		27	80	
Age (years) mean ± SD, years	42.91 ± 10.26	50.09 ± 11.00	0.063	52.15 ± 9.42	48.70 ± 10.40	0.131
Clinical stage(%)						
I	1 (9.1%)	0 (0.0%)	0.061	1 (3.7%)	0 (0.0%)	0.119
II	7 (63.6%)	14 (41.2%)		16 (59.3%)	39 (48.8%)	
III	3 (27.3%)	20 (58.8%)		10 (37.0%)	41 (51.2%)	
Histopathological subtype(%)						
IDC	10 (90.9%)	30 (88.2%)	0.431	26 (96.3%)	69 (86.2%)	0.231
IDC + ILC/+IMPC/+Mucinous cancer	1 (9.1%)	1 (3.0%)		0((0.0%)	8 (10%)	
ILC/IMPC/Mucinous cancer	0 (0.0%)	3 (8.8%)		1 (3.7%)	3 (3.8%)	
Molecular subtype(%)						
Luminal A	2 (18.1%)	6 (17.6%)	0.423	3 (11.1%)	18 (22.5%)	0.309
Luminal B	3 (27.3%)	11 (32.4%)		9 (33.3%)	33 (41.3%)	
Triple negative	4 (36.4%)	5 (14.7%)		4 (14.8%)	9 (11.2%)	
HER2 overexpression	2 (18.1%)	12 (35.3%)		11 (40.7%)	20 (25%)	
ER status(%)						
Positive	6 (54.5%)	17 (50.0%)	0.793	12 (44.4%)	51 (63.7%)	0.078
Negative	5 (45.5%)	17 (50.0%)		15 (55.6%)	29 (36.3%)	
PR status(%)						
Positive	6 (54.5%)	16 (47.1%)	0.666	11 (40.7%)	41 (51.3%)	0.345
Negative	5 (45.5%)	18 (52.9%)		16 (59.3%)	39 (48.7%)	
HER2 status(%)						
Positive	7 (63.6%)	20 (58.8%)	0.777	15 (55.6%)	39 (48.7%)	0.541
Negative	4 (36.4%)	14 (41.2%)		12 (44.4%)	41 (51.3%)	
Ki67(%)						
High	3 (27.3%)	21 (61.8%)	0.046[a]	11 (40.7%)	52 (65%)	0.027[a]
Low	8 (72.7%)	13 (38.2%)		16 (59.3%)	28 (35%)	

ER, estrogen receptor; HER2, human epidermal growth factor receptor 2;IDC, invasive ductal carcinoma; ILC, invasive lobular carcinoma; IMPC, invasive micropapillary carcinoma; PR, progesterone receptor.

[a]p‹0.05

Table 2. Clinical and pathological characteristics of sensitive and insensitive patients in the test and training cohort

	Test cohort		*p*	Training cohort		*p*
	Sensitive	**Insensitive**		**Sensitive**	**Insensitive**	
Amount	32	13		77	30	
Age (years) mean ± SD, years	47.53 ± 11.44	48.62 ± 9.37	0.764	48.83 ± 10.56	50.07 ± 10.83	0.591
Clinical stage(%)						
I	0 (0.0%)	0 (0.0%)	0.893	2 (2.6%)	0 (0.0%)	0.554
II	19 (59.4%)	8 (61.5%)		35 (45.5%)	16 (53.3%)	
III	13 (40.6%)	5 (38.5%)		40 (51.9%)	14 (46.7%)	
Histopathological subtype(%)						
IDC	29 (90.6%)	11 (84.6%)	0.519	72 (93.5%)	23 (76.7%)	0.046[a]
IDC + ILC/+IMPC/+Mucinous cancer	1 (3.1%)	0 (0.0%)		3 (3.9%)	4 (13.3%)	
ILC/IMPC/Mucinous cancer	2 (6.3%)	2 (15.4%)		2 (2.6%)	3 (10%)	
Molecular subtype(%)						
Luminal A	1 (3.1%)	6 (46.2%)	0.002[a]	10 (13.0%)	12 (40.0%)	0.004[a]
Luminal B	11 (34.4%)	2 (15.4%)		36 (46.8%)	7 (23.3%)	
Triple negative	5 (15.6%)	3 (23.0%)		8 (10.4%)	6 (20.0%)	
HER2 overexpression	15 (46.9%)	2 (15.4%)		23 (29.8%)	5 (16.7%)	
ER status(%)						
Positive	12 (37.5%)	8 (61.5%)	0.141	46 (59.7%)	19 (63.3%)	0.732
Negative	20 (62.5%)	5 (38.5%)		31 (40.3%)	11 (36.7%)	
PR status(%)						
Positive	10 (31.2%)	8 (61.5%)	0.060	39 (50.6%)	16 (53.3%)	0.803
Negative	22 (68.8%)	5 (38.5%)		38 (49.4%)	14 (46.7%)	
HER2 status(%)						
Positive	22 (68.8%)	3 (23.1%)	0.005[a]	30 (39.0%)	22 (73.3%)	0.001[a]
Negative	10 (31.2%)	10 (76.9%)		47 (61.0%)	8 (26.7%)	
Ki67(%)						
High	11 (34.4%)	9 (69.2%)	0.033[a]	36 (46.8%)	12 (40.0%)	0.049[a]
Low	21 (65.6%)	4 (30.8%)		41 (53.2%)	18 (60.0%)	

ER, estrogen receptor; HER2, human epidermal growth factor receptor 2;IDC, invasive ductal carcinoma; ILC, invasive lobular carcinoma; IMPC, invasive micropapillary carcinoma; PR, progesterone receptor.

[a]p‹0.05

Table 3. Risk factors for the prediction of NAC sensitivity

Variables	Univariate Logistic		Multivariate Logistic	
	OR(95% CI)	*p*	OR(95% CI)	*p*
Age	0.984 (0.945–1.025)	0.448	NA	NA
Maximum_diameter_of_tumor	1.295 (0.549–3.162)	0.559	NA	NA
Numbers_of_tumor	1.191 (0.326–5.671)	0.804	NA	NA
Mass_NME	1.477 (0.879–2.864)	0.184	NA	NA
Spiculated_margin	0.5 (0.210–1.173)	0.112	NA	NA
Enhancement_kinetics_of_delayed_phase	0.881 (0.401–1.897)	0.748	NA	NA
Minimum_diameter_of_lymph_node	2.8 (1.166–7.170)	0.025[a]	2.8 (1.166–7.710)	0.025[a]
rad_score	NA	NA	2.069 (1.570–2.920)	3.56E-06

CI, confidence interval;;NA, not available.
These variables were removed and the OR3 and P values were not available.
[a]P <0.05.

to 30. LASSO was then employed to identify the optimal subset of features to construct the final model. In consideration of the data imbalance, in the training group, we used the "SMOTE" method to oversample small data sets and obtain balanced data. Finally, these optimal features were used to build the radiomic signatures. In short, the radiomics score (Rad-score) was then calculated for each patient based on the linear combination of the selected features, weighted by their coefficients.

Construction of the nomogram model

The radiomic nomogram model was built by incorporating the optimal clinical factors and radiomic signatures into a multivariate logistic regression model. The nomogram is the visualization of the multivariate logistic regression where each parameter in the nomogram represents a risk factor for predicting pCR or sensitivity. The risk level of each parameter can then be estimated alone and in conjunction with other risk factors to obtain a total risk value. This total risk value represents the probability that the patient will be sensitive to or achieve pCR.

Assessment of the performance of various models and statistical analysis

The calibration of the nomogram was evaluated with a calibration curve. The Hosmer-Lemeshow test was used to assess the goodness-of-fit of a model and the area under the curve (AUC) was calculated for both the training set and validation set to quantify the discrimination performance of the nomogram model. The radiomic nomogram score was calculated for each patient in both sets as well. A decision curve analysis (DCA) was then performed to assess the clinical utility of the nomogram.

Statistical analysis was performed using the R statistical software v. 3.5.1. The "Caret" package was used to preprocess the data and divide it into the training and test groups. The "Glmnet" package was used to perform the LASSO logistic regression model analysis and receiver operating curves (ROCs) were plotted using the "pROC" package. The calibration curve analysis was performed using the "ModelGood" package. Nomogram calibration and construction plots were performed using the "rms" package,

Table 4. Risk factors for the prediction of pCR

Variables	Univariate Logistic		Multivariate Logistic	
	OR(95% CI)	*p*	OR(95% CI)	*p*
Age	0.989 (0.947–1.031))	0.597	NA	NA
Maximum_diameter_of_tumor	0.221 (0.068–0.603)	0.006	0.207	0.032
Numbers_of_tumor	0.592 (0.087–2.450)	0.517	NA	NA
Mass_NME	1.111 (0.691–1.716)	0.643	NA	NA
Spiculated_margin	0.329 (0.102–0.901)	0.042	0.191 (0.043–0.804)	0.021
Enhancement_kinetics_of_delayed_phase	0.684 (0.296–1.563)	0.367	NA	NA
Minimum_diameter_of_lymph_node	0.570 (0.220–1.403)	0.230	NA	NA
rad_score	NA	NA	8.955 (3.827–27.638)	1.01E-05

CI, confidence interval;;NA, not available.
These variables were removed, and the OR and P values were not available. * P <0.05.

Figure 2. (a) Radiomics nomogram for the prediction of NAC sensitivity. Calibration curves of the nomogram model for the training set (b) and validation set (c). Calibration curves indicate the goodness-of fit of the nomogram. The 45 degree gray line indicates the ideal prediction and the dotted lines indicate the predictive performance of the nomogram. A better prediction accuracy of the nomogram is represented as the dotted lines approach the ideal line. ROC curves of various models in the training set (d) and the validation set (e). The nomogram and radiomics signatures show similar performance for prediction while the clinical model shows a poor performance.

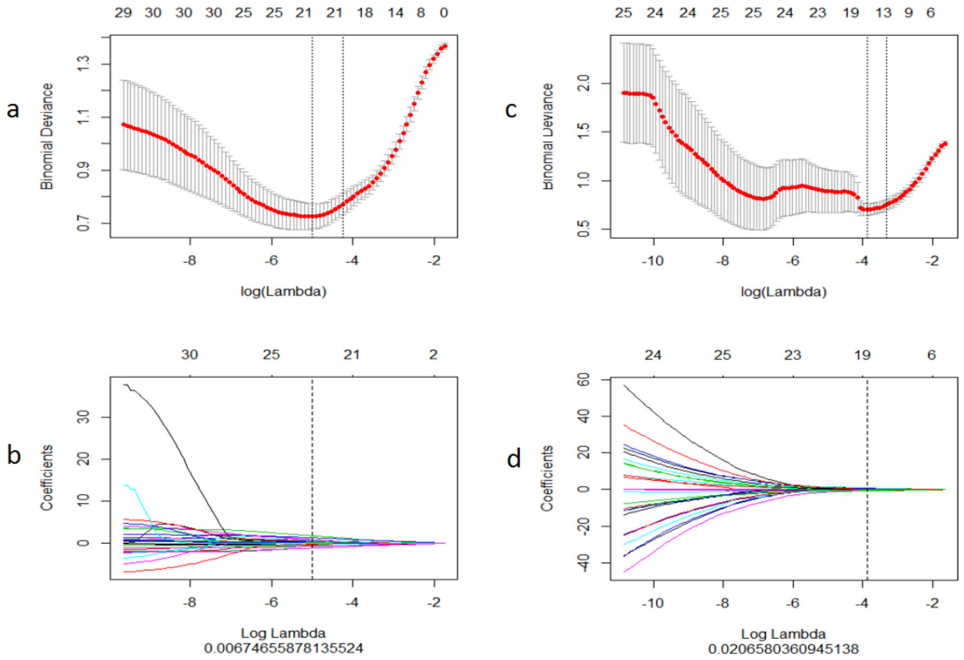

the Hosmer-Lemeshow test was performed using the "generalhoslem" package and DCA was conducted using the "dca.R" package. A p value < 0.05 was considered statistically significant.

RESULTS

Optimal clinical factors and the construction of the clinical factor model

The clinical and pathological characteristics of the patients used for pCR and non-pCR, and for sensitivity and insensitivity comparisons are shown in Tables 1 and 2, respectively. Differences in clinical and pathological characteristics between pCR and non-pCR patients were not significant except for Ki67 in the test and training cohort, while differences between sensitive and insensitive patients were not significant except for molecular subtype, Ki67 and HER2 over expression. Multivariate logistic regression analysis demonstrated that only the minimum diameter of the lymph node was an independent clinical predictor for NAC sensitivity (Table 3, p = 0.025), and that the maximum diameter of the tumor and speculated margin were independent clinical predictors for the possibility of pCR (Table 4, p = 0.032, 0.021, respectively).

The construction of radiomic signatures and the nomogram model and evaluation of performance of various models

396 radiomic features were extracted from each of the T2WI, DWI, DCE-MRI images and were enrolled in the "mRMR" procedure, after which 30 features related to the categorical variable (with minimized redundancy) were retained. The LASSO logistic regression model was then performed on these 30 features to further select the optimal features (Figure 2). The selected features are shown in Supplementary Material 1. Four radiomic signatures were constructed based on the T2WI, DWI, DCE-MRI images and their combination to assess the response to NAC treatment. Four other signatures were built to evaluate the benefit of NAC. The selected clinical factors were used to construct the nomogram model. The combined radiomic signature and nomogram model displayed a stronger predictive efficacy in the training (AUC 0.91, 0.92, 95% CI, 0.85–0.96, 0.86–0.98) and validation set (AUC 0.93, 0.91, 95% CI, 0.86–1.00, 0.82–1.00) compared to clinical factor model (AUC 0.74, 0.64, 95% CI, 0.64–0.84, 0.46–0.82) for NAC sensitivity and possibility of pCR (Figures 3 and 4). The clinical factor model exhibited very poor diagnostic performance between the radiomics signature and nomogram model and revealed no significant difference (Tables 5 and 6). Rad-scores were calculated by adding the selected features, weighted by their coefficients. The clinical utility of the Rad-scores were confirmed by the DCA (Figure 5) which showed that the radiomics nomogram model exhibited a better overall net benefit in the prediction of NAC sensitivity and pCR probability.

DISCUSSION

The results presented here confirm that most patients can benefit from NAC treatment to various degrees and that NAC has gained importance for the standard treatment of breast cancer.

Figure 3. **(a)** Radiomics nomogram for the prediction of the probability of achieving pCR. Calibration curves of the nomogram in the training set **(b)** and the validation set **(c).** Calibration curves indicate the goodness-of fit of the nomogram. The 45 degree gray line indicates the ideal prediction, and the dotted lines indicate the predictive performance of the nomogram. A better prediction accuracy of the nomogram is represented as the dotted lines approach the ideal line. ROC curves of various models in the training set **(d)** and the validation set **(e).** The nomogram and radiomics signatures show similar performance for prediction while the clinical model shows a poor performance.

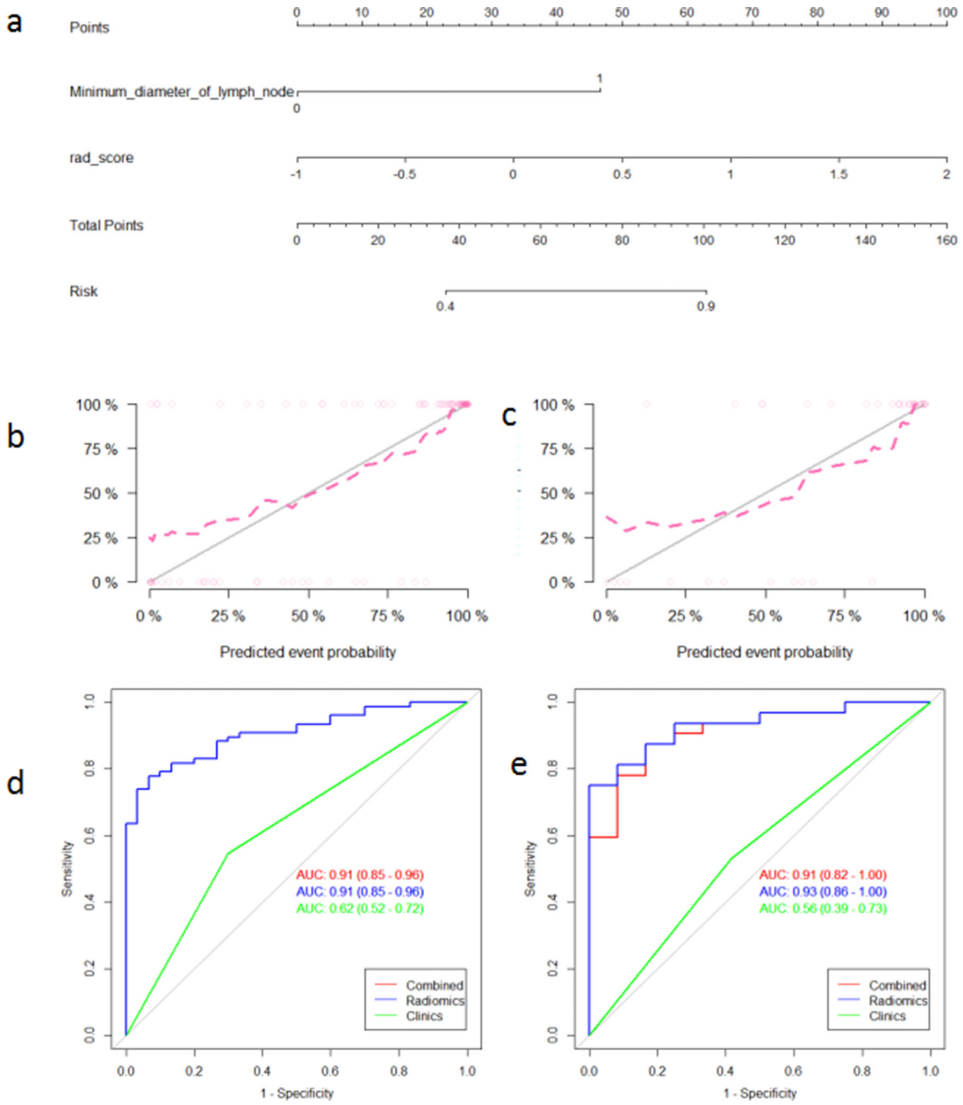

Therapeutic assessment is a key factor in the determination of treatment decisions.[21–23] Finding an appropriate method for predicting the sensitivity to NAC and whether patients could achieve pCR before surgery would facilitate the following treatment decision: undergo NAC without surgery or undergo surgery without NAC. For example, patients who are predicted to achieve pCR may avoid surgery in the future if such findings are supported by big data or clinical trials, while those who are predicted to be insensitive to NAC should prefer surgical treatments as they would benefit less from NAC compared with toxicity. Additionally, the sensitivity to NAC could guide the selection of subsequent adjuvant chemotherapy drugs as it can be considered a drug-sensitivity test before surgery. The efficacy of NAC was clinically estimated through imaging analyses according to the RECIST v. 1.1 toolbox before surgery without radiomics and was ultimately confirmed via pathological evaluation according to the Miller-Payne grading system.[24–26] With radiomics we can predict the treatment response using only the pre-treatment MRI images, which is a major advantage compared to other methods. Therefore, it is crucial to identify whether radiomics signatures and/or a nomogram model based on non-invasive pre-treatment MR images can yield a more accurate prediction of the benefits of NAC treatment.

In the current study, we explored the association between the response and benefit of NAC treatment with pre-treatment MRI markers. Specifically, we automatically extracted quantitative features from various MRI scans and constructed different machine learning models based on the selected clinical factors and multiparametric MRI radiomic signatures. We evaluated

Figure 4. Decision curve analysis of various models for NAC sensitivity (a) and probability of achieving pCR (b), respectively. The x-axis indicates the threshold probability and the y-axis indicates the net benefit. The red and green lines represent the net benefit of the nomogram and clinical factor models, respectively. The radiomics model shows the highest net benefit.

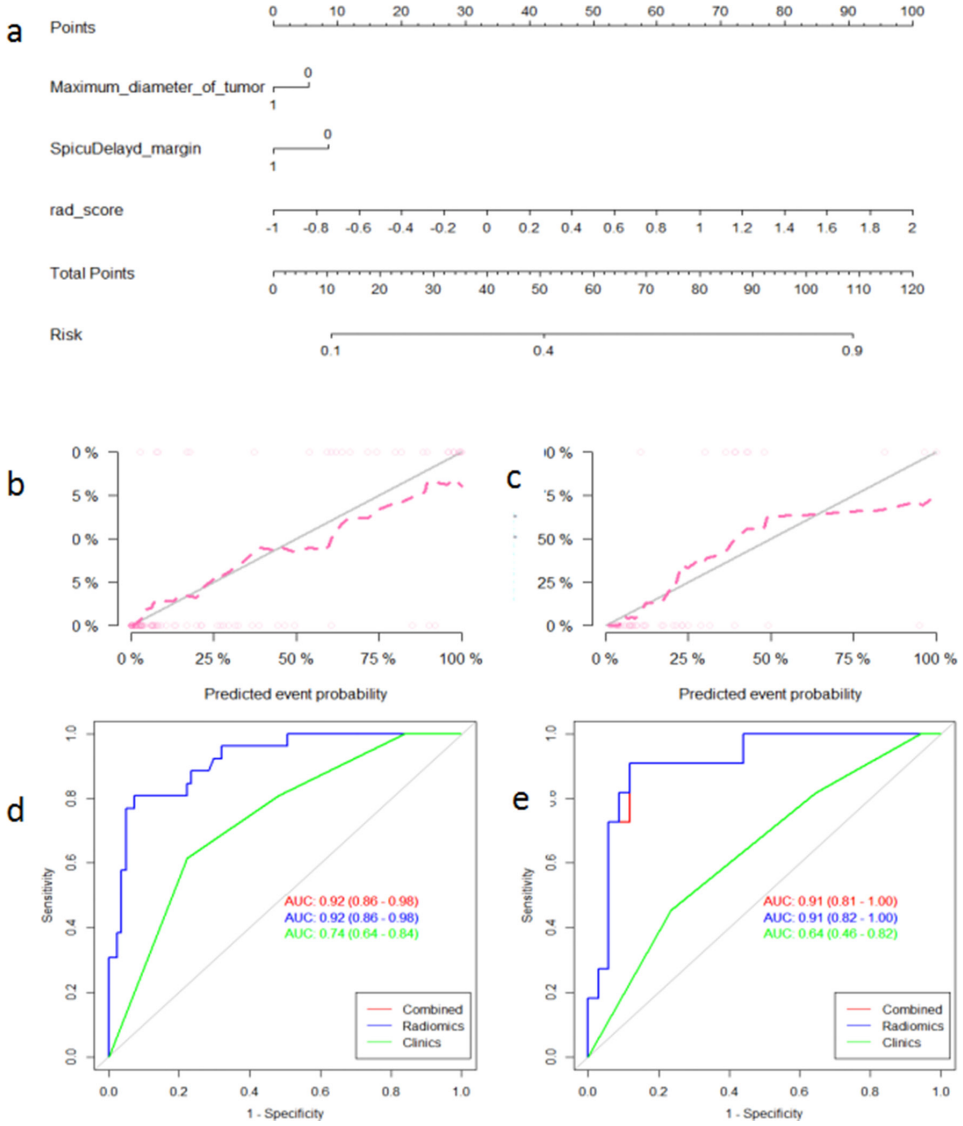

the ability of radiomic signatures, based on pre-treatment MRI, to predict the response to NAC instead of simply analyzing the characteristics of MRI images before and after NAC, which follows the RECIST 1.1 criteria. We assessed the performance of these models in an independent validation set and obtained an AUC of more than 0.90 for identifying, before surgery, which patient would be sensitive or insensitive to NAC and which patient would reach pCR.

Unlike previous studies that have explored radiomics signatures based on only one imaging scan/modality, we utilized four radiomics signatures and compared the performance of all of them.[21,27–30] The results of our study demonstrated that among the radiomics signatures based on T2WI, DWI, DCE-MRI and the combination of these three, the combined signature performed best for predicting NAC sensitivity and the possibility of achieving pCR. Clinical and pathological characteristics of patients showed no significance differences except for Ki67 between pCR and non-pCR patients, and molecular subtype, Ki67 and HER2 overexpression between sensitive and insensitive patients, which is consistent with a previous study. In particular, molecular subtype and Ki67 have been proven to be associated with the prognosis of breast cancer.[25] Clinical factors were then added to the combined radiomics signature to build the nomogram model. Only the minimum diameter of the lymph node, the maximum diameter of the tumor and the speculated margin were included in the multivariate logistic regression model for the prediction of NAC sensitivity and possibility of achieving pCR. The radiomics signature and nomogram model displayed a strong predictive ability with an AUC reaching greater than 0.90. This is in contrast to the model comprised of only clinical factors that displayed a weaker predictive ability and produced an AUC of less than 0.70, which is consistent with previous studies.[31–34] Nevertheless, the clinical factors model performed so poorly,

Table 5. Diagnostic performance of the radiomic signatures and the nomogram for the prediction of NAC sensitivity

	Training set (n = 107)						Validation set (n = 45)					
	Accuracy	Sensitivity	Specificity	PPV	NPV	AUC(95% CI)	Accuracy	Sensitivity	Specificity	PPV	NPV	AUC(95% CI)
Radiomics signature	0.822	0.933	0.779	0.622	0.968	0.91 (0.85–0.96)	0.818	1	0.75	0.6	1	0.91 (0.82–1.00)
Radiomics nomogram	0.822	0.933	0.779	0.622	0.968	0.91 (0.85–0.96)	0.818	1.000	0.750	0.600	1.000	0.93 (0.86–1.00)

CI, confidence interval; PPV, positive prediction value; NPV, negative prediction value

Table 6. Diagnostic performance of radiomic signatures and the nomogram for the prediction of pCR

	Training set (n = 107)						Validation set (n = 45)					
	Accuracy	Sensitivity	Specificity	PPV	NPV	AUC(95% CI)	Accuracy	Sensitivity	Specificity	PPV	NPV	AUC(95% CI)
Radiomics signature	0.897	0.926	0.808	0.938	0.778	0.92 (0.86–0.98)	0.889	0.882	0.909	0.968	0.714	0.91 (0.81–1.00)
Radiomics nomogram	0.897	0.926	0.808	0.938	0.778	0.92 (0.86–0.98)	0.889	0.882	0.909	0.968	0.714	0.91 (0.82–1.00)

CI, confidence interval; PPV, positive prediction value; NPV, negative prediction value

Figure 5. The T2WI (a), DWI (b), initial enhanced (c) and delayed enhanced (d) images for radiomic analysis in a 56-year-old patient with a luminal A invasive ductal carcinoma in the left breast with manual region of interest (ROI) placement.

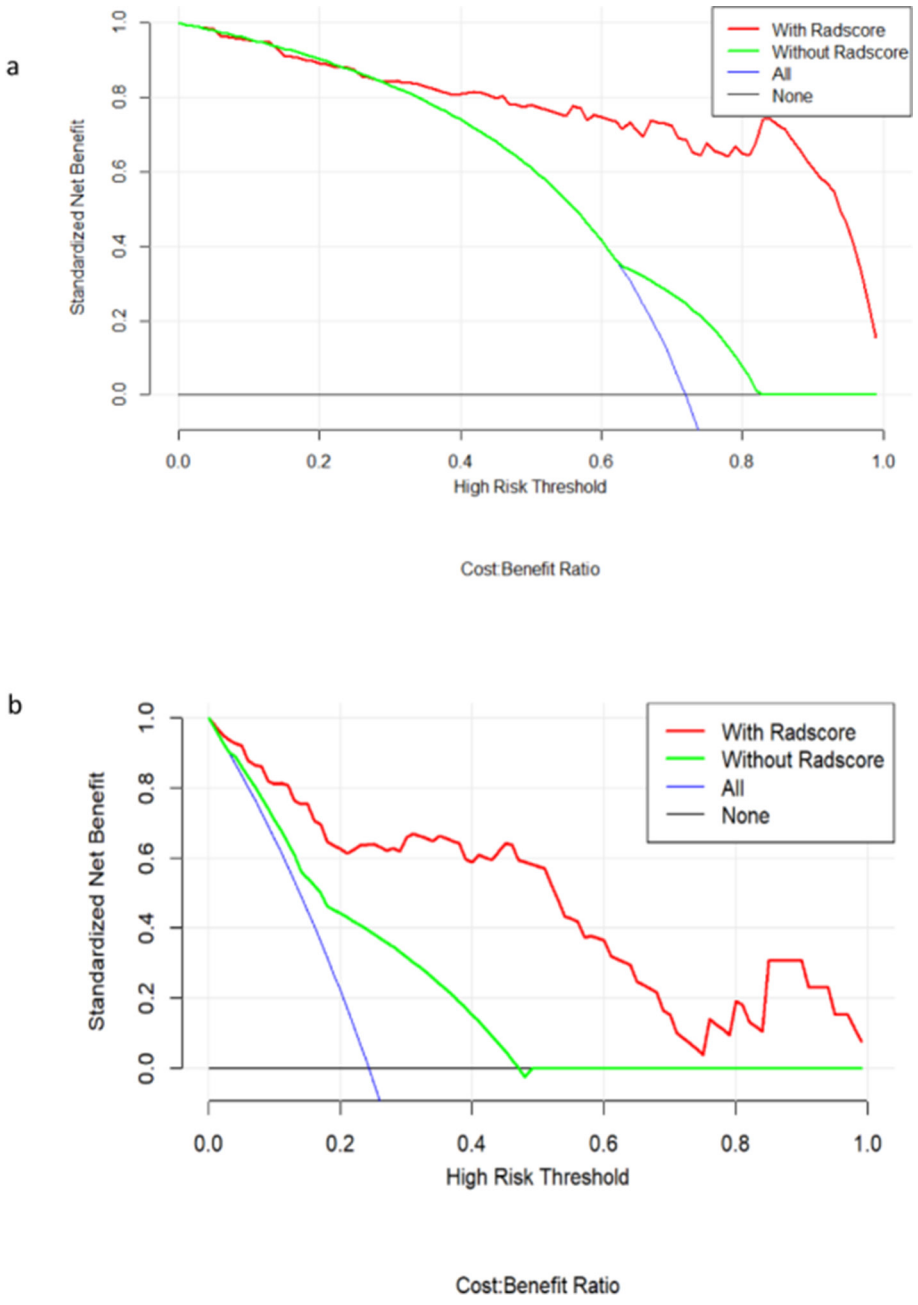

likely due to the variability across molecular subtypes, that the combined radiomics signature and nomogram model produced almost the same accuracy, sensitivity, specificity, PPV, and NPV values. This could have been caused by the difference in the selection of clinical factors and small sample size. Therefore, a bigger cohort and a more comprehensive study is needed to validate our results.

Our study has various limitations. Firstly, this study was a single-center retrospective study and may not be consistent with or able to be applied to data/patients from other institutions. Secondly, further independent validation is required due to the relatively limited MR protocols and small cohort size. Furthermore, we excluded those patients with multi focal lesions which made the study less representative of the full patient population. In addition, ROIs were drawn on a selected section of two-dimensional images for simplicity and consistency rather than on more complicated three-dimensional images which could be more accurate but also much more variable. Finally, there is no definite standard for the drawing of ROIs of non-mass-like lesions. It is therefore difficult to mark the margin of these lesions and reduces the reproducibility and reliability of intra-observer results. In the future, multi-center and multi-focal studies with larger cohort size and more abundant information is needed to confirm our results.

CONCLUSION

In conclusion, our study demonstrates that radiomic signatures and a nomogram model are non-invasive predictive tools that show much more favorable predictive accuracies for the response type and benefit of NAC treatment before surgery compared with clinical factors and simple imaging features. These tools have been gradually used for the differential diagnosis of benign and malignant tumors and can also provide guidance of subsequent treatment. In the future, this technique can be used for the prediction of prognoses and molecular subtypes. Radiomics is an emerging field that is believed to bring us more benefits in the future.

COMPETING INTERESTS

The author states no potential conflicts of interest.

ETHICS APPROVAL

This retrospective study was approved by the Institutional Review Board of the Affiliated Hospital of Qingdao University.

DISCLOSURE

Written informed consent was provided by all individuals before participation.

REFERENCES

1. Nie P, Yang G, Wang Z, Yan L, Miao W, Hao D, et al. A CT-based radiomics nomogram for differentiation of renal angiomyolipoma without visible fat from homogeneous clear cell renal cell carcinoma. *Eur Radiol* 2020; **30**: 1274–84. doi: https://doi.org/10.1007/s00330-019-06427-x
2. Gillies RJ, Kinahan PE, Hricak H. Radiomics: images are more than pictures, they are data. *Radiology* 2016; **278**: 563–77. doi: https://doi.org/10.1148/radiol.2015151169
3. Liu Z, Li Z, Qu J, Zhang R, Zhou X, Li L, et al. Radiomics of multiparametric MRI for pretreatment prediction of pathologic complete response to neoadjuvant chemotherapy in breast cancer: a multicenter study. *Clin Cancer Res* 2019; **25**: 3538–47. doi: https://doi.org/10.1158/1078-0432.CCR-18-3190
4. Berruti A, Generali D, Kaufmann M, Puztai L, Curigliano G, Aglietta M, et al. International expert consensus on primary systemic therapy in the management of early breast cancer: highlights of the fourth Symposium on primary systemic therapy in the management of operable breast cancer, Cremona, Italy (2010. *J Natl Cancer Inst Monogr* 2011; **2011**: 147–51. doi: https://doi.org/10.1093/jncimonographs/lgr037
5. Iotti V, Ravaioli S, Vacondio R, Coriani C, Caffarri S, Sghedoni R, et al. Contrast-Enhanced spectral mammography in neoadjuvant chemotherapy monitoring: a comparison with breast magnetic resonance imaging. *Breast Cancer Res* 2017; **19**: 106. doi: https://doi.org/10.1186/s13058-017-0899-1
6. Le-Petross HT, Lim B. Role of Mr imaging in neoadjuvant therapy monitoring. *Magn Reson Imaging Clin N Am* 2018; **26**: 207–20. doi: https://doi.org/10.1016/j.mric.2017.12.011
7. Untch M, Konecny GE, Paepke S, von Minckwitz G. Current and future role of neoadjuvant therapy for breast cancer. *Breast* 2014; **23**: 526–37. doi: https://doi.org/10.1016/j.breast.2014.06.004
8. Braman NM, Etesami M, Prasanna P, Dubchuk C, Gilmore H, Tiwari P, et al. Intratumoral and peritumoral radiomics for the pretreatment prediction of pathological complete response to neoadjuvant chemotherapy based on breast DCE-MRI. *Breast Cancer Res* 2017; **19**: 57. doi: https://doi.org/10.1186/s13058-017-0846-1
9. Lambin P, Leijenaar RTH, Deist TM, Peerlings J, de Jong EEC, van Timmeren J, et al. Radiomics: the bridge between medical imaging and personalized medicine. *Nat Rev Clin Oncol* 2017; **14**: 749–62. doi: https://doi.org/10.1038/nrclinonc.2017.141
10. Cortazar P, Geyer CE. Pathological complete response in neoadjuvant treatment of breast cancer. *Ann Surg Oncol* 2015; **22**: 1441–6. doi: https://doi.org/10.1245/s10434-015-4404-8
11. Broglio KR, Quintana M, Foster M, Olinger M, McGlothlin A, Berry SM, et al. Association of pathologic complete response to neoadjuvant therapy in HER2-positive breast cancer with long-term outcomes: a meta-analysis. *JAMA Oncol* 2016; **2**: 751–60. doi: https://doi.org/10.1001/jamaoncol.2015.6113
12. Liu Y-H, Ye J-M, Xu L, Huang Q-Y, Zhao J-X, Duan X-N, et al. Effectiveness of dynamic contrast-enhanced magnetic resonance imaging in evaluating clinical responses to neoadjuvant chemotherapy in breast cancer. *Chin Med J* 2011; **124**: 194–8.
13. Chen S, Liu Y, Ouyang Q-W, Huang L, Luo R-C, Shao Z-M. Clinical and pathological response to neoadjuvant chemotherapy based on primary tumor reduction is correlated to survival in hormone receptor-positive but not hormone receptor-negative locally advanced breast cancer. *Ann Surg Oncol* 2015; **22**: 32–9. doi: https://doi.org/10.1245/s10434-014-3894-0
14. Yu N, Leung VWY, Meterissian S. Mri performance in detecting pCR after neoadjuvant chemotherapy by molecular subtype of breast cancer. *World J Surg* 2019; **43**: 2254–61. doi: https://doi.org/10.1007/s00268-019-05032-9
15. Saccarelli CR, Bitencourt AGV, Morris EA. Breast cancer screening in high-risk women: is MRI alone enough? *J Natl Cancer Inst* 2019;.
16. Koh J, Park AY, Ko KH, Jung HK. Can enhancement types on preoperative MRI reflect prognostic factors and surgical outcomes in invasive breast cancer? *Eur Radiol* 2019; **29**: 7000–8. doi: https://doi.org/10.1007/s00330-019-06236-2
17. Hilal T, Covington M, Kosiorek HE, Zwart C, Ocal IT, Pockaj BA, et al. Breast MRI phenotype and background parenchymal enhancement may predict tumor response to neoadjuvant endocrine therapy. *Breast J* 2018; **24**: 1010–4. doi: https://doi.org/10.1111/tbj.13101
18. Mazurowski MA. Radiogenomics: what it is and why it is important. *J Am Coll Radiol* 2015; **12**: 862–6. doi: https://doi.org/10.1016/j.jacr.2015.04.019
19. Chamming's F, Ueno Y, Ferré R, Kao E, Jannot A-S, Chong J, et al. Features from computerized texture analysis of breast cancers at pretreatment MR imaging are associated with response to neoadjuvant chemotherapy. *Radiology* 2018; **286**: 412–20. doi: https://doi.org/10.1148/radiol.2017170143
20. Yu Q, Huang K, Zhu Y, Chen X, Meng W. Preliminary results of computer-aided diagnosis for magnetic resonance imaging of solid breast lesions. *Breast Cancer Res Treat*

2019; **177**: 419–26. doi: https://doi.org/10.1007/s10549-019-05297-7
21. Leithner D, Bernard-Davila B, Martinez DF, Horvat JV, Jochelson MS, Marino MA, et al. Radiomic signatures derived from diffusion-weighted imaging for the assessment of breast cancer receptor status and molecular subtypes. *Mol Imaging Biol* 2020; **22**: 453–61. doi: https://doi.org/10.1007/s11307-019-01383-w
22. Cain EH, Saha A, Harowicz MR, Marks JR, Marcom PK, Mazurowski MA. Multivariate machine learning models for prediction of pathologic response to neoadjuvant therapy in breast cancer using MRI features: a study using an independent validation set. *Breast Cancer Res Treat* 2019; **173**: 455–63. doi: https://doi.org/10.1007/s10549-018-4990-9
23. Tan W, Yang M, Yang H, Zhou F, Shen W. Predicting the response to neoadjuvant therapy for early-stage breast cancer: tumor-, blood-, and imaging-related biomarkers. *Cancer Manag Res* 2018; **10**: 4333–47. doi: https://doi.org/10.2147/CMAR.S174435
24. Wu S, Zheng J, Li Y, Yu H, Shi S, Xie W, et al. A Radiomics nomogram for the preoperative prediction of lymph node metastasis in bladder cancer. *Clin Cancer Res* 2017; **23**: 6904–11. doi: https://doi.org/10.1158/1078-0432.CCR-17-1510
25. Xiong Q, Zhou X, Liu Z, Lei C, Yang C, Yang M, et al. Multiparametric MRI-based radiomics analysis for prediction of breast cancers insensitive to neoadjuvant chemotherapy. *Clin Transl Oncol* 2020; **22**: 50–9. doi: https://doi.org/10.1007/s12094-019-02109-8
26. Nam KJ, Park H, Ko ES, Lim Y, Cho H-H, Lee JE. Radiomics signature on 3T dynamic contrast-enhanced magnetic resonance imaging for estrogen receptor-positive invasive breast cancers: preliminary results for correlation with Oncotype DX recurrence scores. *Medicine* 2019; **98**: e15871. doi: https://doi.org/10.1097/MD.0000000000015871
27. Chai R, Ma H, Xu M, Arefan D, Cui X, Liu Y, et al. Differentiating axillary lymph node metastasis in invasive breast cancer patients: a comparison of radiomic signatures from multiparametric breast Mr sequences. *J Magn Reson Imaging* 2019; **50**: 1125–32. doi: https://doi.org/10.1002/jmri.26701
28. Crivelli P, Ledda RE, Parascandolo N, Fara A, Soro D, Conti M. A new challenge for radiologists: Radiomics in breast cancer. *Biomed Res Int* 2018; **2018**: 1–10. doi: https://doi.org/10.1155/2018/6120703
29. Vriens BEPJ, de Vries B, Lobbes MBI, van Gastel SM, van den Berkmortel FWPJ, Smilde TJ, et al. Ultrasound is at least as good as magnetic resonance imaging in predicting tumour size post-neoadjuvant chemotherapy in breast cancer. *Eur J Cancer* 2016; **52**: 67–76. doi: https://doi.org/10.1016/j.ejca.2015.10.010
30. Zhi W, Liu G, Chang C, Miao A, Zhu X, Xie L, et al. Predicting treatment response of breast cancer to neoadjuvant chemotherapy using ultrasound-guided diffuse optical tomography. *Transl Oncol* 2018; **11**: 56–64. doi: https://doi.org/10.1016/j.tranon.2017.10.011
31. An YY, Kim SH, Kang BJ, Lee AW. Treatment response evaluation of breast cancer after neoadjuvant chemotherapy and usefulness of the imaging parameters of MRI and PET/CT. *J Korean Med Sci* 2015; **30**: 808–15. doi: https://doi.org/10.3346/jkms.2015.30.6.808
32. Zinn PO, Mahajan B, Majadan B, Sathyan P, Singh SK, Majumder S, et al. Radiogenomic mapping of edema/cellular invasion MRI-phenotypes in glioblastoma multiforme. *PLoS One* 2011; **6**: e25451. doi: https://doi.org/10.1371/journal.pone.0025451
33. Yamamoto S, Maki DD, Korn RL, Kuo MD. Radiogenomic analysis of breast cancer using MRI: a preliminary study to define the landscape. *AJR Am J Roentgenol* 2012; **199**: 654–63. doi: https://doi.org/10.2214/AJR.11.7824
34. Mazurowski MA, Zhang J, Grimm LJ, Yoon SC, Silber JI. Radiogenomic analysis of breast cancer: luminal B molecular subtype is associated with enhancement dynamics at MR imaging. *Radiology* 2014; **273**: 365–72. doi: https://doi.org/10.1148/radiol.14132641